

Assignment of ^1H and ^{13}C Nuclear Magnetic Resonances of Ganglioside G_{A1}

Kyungik Lee, Gilja Jhon[†], Gyungilm Rhyu[†],
Eunjung Bang[‡], Byongseok Choi[§], and Yangmee Kim^{*}

Department of Chemistry, Konkuk University, Seoul 133-701, Korea

[†]*Department of Chemistry, Ewha Womans University, Seoul 120-750, Korea*

[‡]*Department of Material's Analysis, National Industrial Technology Institute, Kwacheon 427-010, Korea*

[§]*Korea Basic Science Institute, Seoul 136-701, Korea*

^{*}*Department of Chemistry, Korea Advanced Institute of Science and Technology, Taejon 305-701, Korea*

Received June 19, 1995

Investigation of the structures of the gangliosides has proven to be very important in the understanding of their biological roles such as regulation of differentiation and growth of cells. We used nuclear magnetic resonance spectroscopy in order to investigate the structure of G_{A1} . In order to do this, the assignment of spectra is a prerequisite. Since G_{A1} does not have polar sialic acid, the spectral overlap is severe. In order to solve this problem, we use 2D NMR spectroscopy and heteronuclear $^1\text{H}/^{13}\text{C}$ correlated spectroscopy in this study. Here, we report the complete assignment of the proton and the carbon spectra of the G_{A1} in $\text{DMSO-d}_6\text{-D}_2\text{O}$ (98 : 2, v/v). These assignments will be useful for interpreting ^1H and ^{13}C NMR data from uncharacterized oligosaccharides and for determining the linkage position, the number of sugar rings, and the sequence of new ganglioside. Amide proton in ring III shows many interring NOEs and has intramolecular hydrogen bonding. This appears to be an important factor in tertiary folding of G_{A1} . Based on this assignment, determination of three dimensional structure of G_{A1} will be carried out. Studies on the conformational properties of G_{A1} may lead to a better understanding of the molecular basis of its functions.

Introduction

Gangliosides are sialic acid containing glycosphingolipids, found in the plasma membrane of animal cells, being particularly abundant in the nervous system.^{1,2} They are asymmetrically located in the outer face of the membrane with the complex carbohydrate head groups, which extend beyond the surface of the cell interacting with a variety of external ligand. Gangliosides may be included in the process of specific recognition of signal molecules at the membrane surface and signal transduction through the membrane.³ Due to the considerable evidence that gangliosides may function as membrane receptors, antigenic determinants, and cell-cell recognition sites, there is a growing need to determine the three-dimensional structures of gangliosides.

Recent interest in asialo- G_{M1} (G_{A1} ; $\beta\text{D-Gal}(1-3)\beta\text{D-GalNAc}(1-4)\beta\text{D-Gal}(1-4)\beta\text{D-GlcCer}$) arises from the finding that it is a cell-surface marker of mouse, natural-killer cells,^{4,5} and it may be associated with natural, cell-mediated cytotoxicity.⁶ It may also serve as a differentiation antigen of mouse⁷ and rat thymocytes.⁸ In addition, G_{A1} appears to be a cell-surface marker of leukemic cells from patients having acute, lymphoblastic leukemia.⁹ Since G_{A1} is more antigenic than most of the gangliosides, and is also capable of eliciting highly specific antibodies,¹⁰ studies of its structures on the molecular level is necessary to enable studies of its interaction with immunoglobulins to proceed.

At present the only method with which to determine ganglioside solution structure with accuracy is high resolution NMR spectroscopy. Recently conformations of some ganglio-

sides were determined by NMR spectroscopy and molecular modeling.¹¹⁻¹⁴ In order to determine the three dimensional structure of ganglioside by NMR spectroscopy, the assignment of spectrum is a prerequisite. However, there are difficulties in completing the assignment of nuclear magnetic resonances of ganglioside because of the severe spectral overlap. All methine resonances of rings, except anomeric resonances, fall within a 1 ppm chemical shift range. This is a problem common to all oligosaccharide spectra. In order to solve this problem, we use 2D NMR spectroscopy and heteronuclear $^1\text{H}/^{13}\text{C}$ correlated spectroscopy in this study. Here, we report the assignment of the proton and carbon spectra of the G_{A1} . Based on this assignment, determination of three dimensional structure of G_{A1} will be carried out.

Experimental

98% pure G_{A1} from bovine brain was purchased from Sigma. Sample was deuterium-exchanged by repeated lyophilization from $\text{DMSO-d}_6\text{-D}_2\text{O}$ mixture and finally dissolved in 0.4 mL of $\text{DMSO-d}_6\text{-D}_2\text{O}$ (98 : 2, v/v) solvent for NMR spectroscopy and made to 7 mM in the nmr tube. Upon storage at a cold temperature after each NMR experiment, G_{A1} in solution is found to be stable for months, with no signs of degradation. Chemical shifts are expressed relative to the DMSO signal (^1H at 2.49 ppm, ^{13}C at 39.5 ppm).

All the phase sensitive two dimensional experiments such as DQF-COSY,¹⁵ TOCSY,¹⁶ and NOESY¹⁷ experiments were performed using TPPI method, *i.e.*, time-proportional phase incrementation.¹⁸ For these experiments, 256-400 transients with 2 K complex data points were collected for each increment with a relaxation delay of 1.5 sec between successive

[†]To whom correspondences should be addressed.

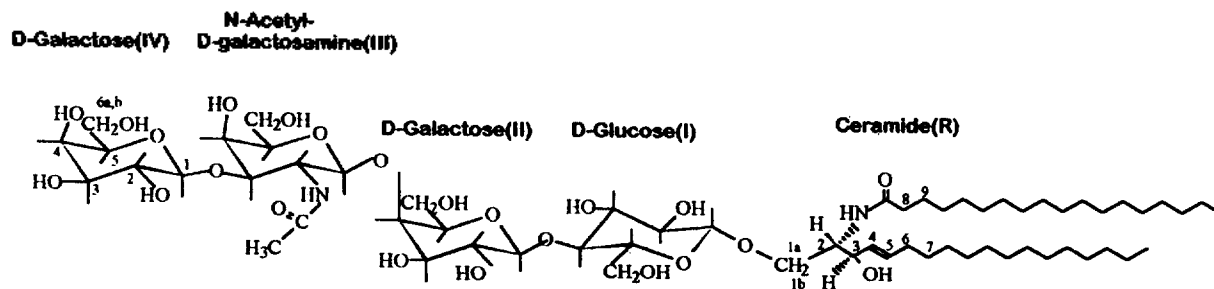


Figure 1. Primary structure of G_{A1} with symbolism and numbering.

transients and the data along the t_1 dimension were zero-filled to 1 K before 2D-Fourier transformation. Data were recorded with 64 scans for each t_1 increment with a spectral width of 4504.5 Hz in both dimension. For the magnitude COSY^{19,20} and RELAY²¹ experiments, 400 transients with 4 K complex data points were collected for each increment and the data along the t_1 dimension were zero-filled to 2 K. Data were recorded with 32 scans for each t_1 increment with a spectral width of 3268.0 Hz. Prior to Fourier transformation, shifted skewed sine bell weighting function and zero filling were applied to give a final data matrix of 2048 × 2048 real points. HMQC (heteronuclear multiple-quantum coherence spectroscopy)²² experiments were performed in the phase sensitive mode using TPPI method, 256 FIDs of 2048 complex points were acquired. HMBC (heteronuclear multiple-bond correlation spectroscopy)²³ experiments were performed in the magnitude mode and a total of 256 FIDs were acquired. Both HMQC and HMBC experiments were conducted with the ^1H spectral width set to 3521.1 Hz and the ^{13}C spectral width set to 23770.9 Hz. TOCSY pulse program used a 95 msec, MLEV-17 spin-lock mixing pulse. Mixing times of 150-250 msec were used for NOESY and ROESY²⁴ experiments.

The 1D nOe values were obtained by selective inversion recovery in the difference mode. In order to see the nOes between unexchanged-NH and the other protons, sample was dissolved in 100% DMSO. Irradiation times and pulse intervals were greater than 5 times the longest T_1 for the signals of G_{A1} . Mixing time of 600 msec was used for nOe transfer.

All spectra were recorded at 303 K on a Bruker AMX-500 spectrometer in Inter-University Center for Natural Science Research Facilities in Seoul National University and Korea Basic Science Institute. All NMR spectra were processed off-line using the FELIX software package²⁵ on SGI workstation in our laboratory.

Results and Discussion

As shown in Figure 1a, G_{A1} is composed of four sugar rings and ceramide and lack of sialic acid. Figure 2a shows the ^1H 1D spectrum of G_{A1} in 100% DMSO and Figure 2b shows that in DMSO- d_6 - D_2O (98 : 2, v/v) solvent. This figure summarizes the assignment of ^1H resonances. Because G_{A1} has most of the resonances of rings between 3 ppm and 4 ppm, the assignment of the proton spectrum is very difficult. Since by exchange of hydroxyl and amide protons, the proton spectrum becomes much simpler as shown in Figure

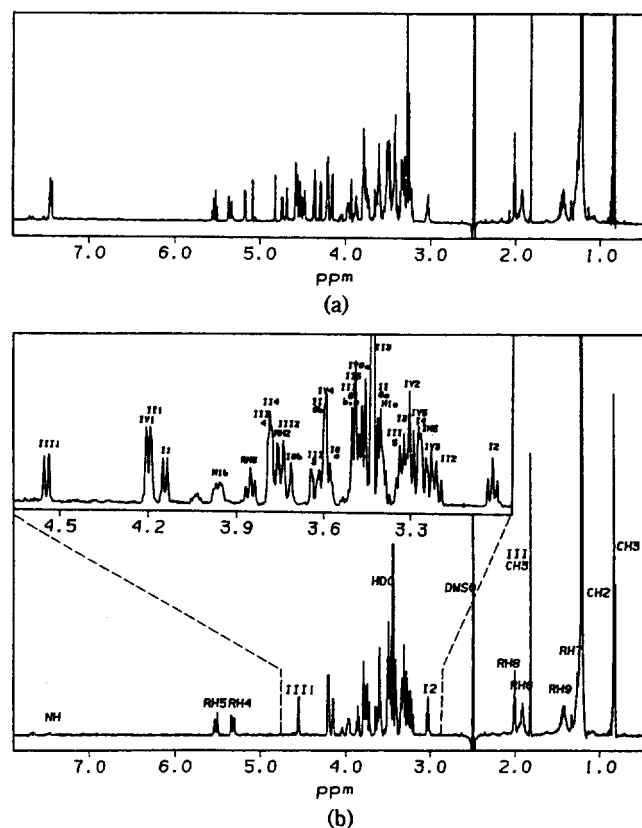


Figure 2. (a) Proton NMR spectrum of 7 mM G_{A1} in 100% DMSO obtained at 500 MHz, at 303 K. (b) proton NMR spectrum of G_{A1} in DMSO- d_6 - D_2O (98 : 2, v/v) obtained at 500 MHz at 303 K. Amide protons and hydroxy protons are exchanged with D_2O .

2b, all the assignment in this report was done on the spectra acquired on the deuterium exchanged sample. ^1H NMR spectrum of G_{A1} shows four resolved anomeric resonances between 4.142 and 4.547 ppm. COSY, RELAY, TOCSY, and NOESY experiments made it possible to assign the resonances from H1 to H4 in the four rings easily. Even though the assignment was not completed by correlating proton-proton through-bond connectivities and through-space connectivities, proton resonances show well resolved correlations to the ^{13}C resonances in HMQC and HMBC spectra. The chemical shifts of protons up to H6b are confirmed and chemical shifts of some H5, H6a, and H6b which are not assigned by proton NMR experiments are assigned by HMQC and

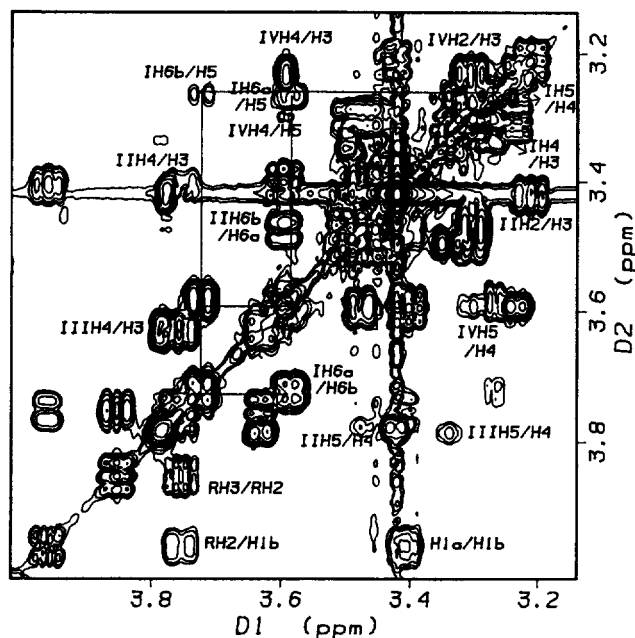


Figure 3. COSY spectrum of 7 mM G_{A1} in $DMSO-d_6-D_2O$ (98 : 2, v/v) at 303 K, at 500 MHz. Solid line shows the through-bond connectivities of ring I.

HMBC experiments. HMQC and HMBC experiments offer a variety of ways to identify all directly bonded and long-range carbon-proton pairs in G_{A1} and allow to complete the assignment of 1H and ^{13}C spectrum.

For ring I, starting with well resolved anomeric resonances at 4.142 ppm, resonances up to H6b are assigned in the magnitude COSY spectrum as shown in Figure 3. As shown in Figure 4b and 4c, the solid lines in TOCSY and NOESY spectra show through-bond connectivities and through-space connectivities between H1 and the other protons in ring I. HMBC spectrum shows the IIC1/IH4 coupling peak across the glycosidic bond and confirms the assignment of H4 resonance. Since the chemical shift of H5 is very close to that of H4, the cross peaks correlated with H5 in every proton 2D spectra are complicated. However, the C5/H5 cross peak in HMQC spectrum make it possible to assign H5 resonance. Chemical shifts of H6a and H6b are assigned by C6/H6a and C6/H6b peaks in HMQC spectrum as shown in Figure 5a. Among the two H6 protons, one in upfield is named as H6a and the other in downfield is named as H6b.

In the case of ring II, anomeric resonance is overlapped with that of ring IV. However, as shown in Figure 4a, the IHH2/H1 cross peak is well resolved in DQF-COSY spectrum and resonances up to H4 are assigned by COSY, RELAY and TOCSY spectra and also confirmed by HMQC and HMBC spectra. Especially, chemical shift of H4 is confirmed by the IIC1/IHH4 correlation across the glycosidic bond in HMBC spectrum. H6a in ring II was assigned by COSY and RELAY spectra. As shown in Figure 5a, the C6/H6a and the C6/H6b cross peaks appear in HMQC spectrum. The C5/H6a and the C5/H6b cross peaks in the HMBC spectrum make it possible to assign the chemical shifts of H6a and H6b in ring II.

Cross peak connectivities from the most downfield anome-

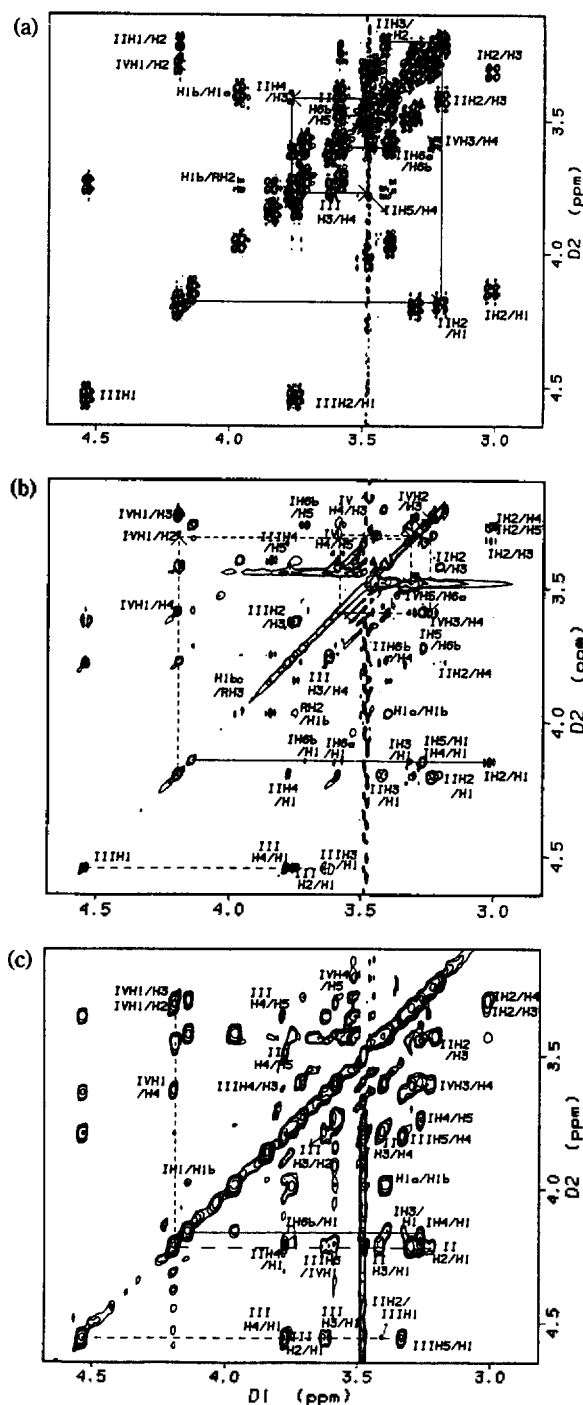


Figure 4. (a) Absorption mode 1H DQF-COSY spectrum of 7 mM G_{A1} in $DMSO-d_6-D_2O$ (98 : 2, v/v) at 303 K, at 500 MHz. A contour plot contains most of the ring proton connectivities. Solid line shows the through-bond connectivities of ring II. Spectrum is plotted with negative and positive components of the cross peaks at a level slightly above noise. As a result, weak cross peaks are not visible. (b) A contour plot of the same region of TOCSY spectrum with 98 msec mixing time. Dotted line (---) shows the through-bond connectivities of ring IV. The other lines show the connectivities between IIIH1, IH1 and the other protons in ring III and ring I. (c) A contour plot of the same region of the NOESY spectrum with 250 msec mixing time. Each line shows the through-space connectivities between anomeric protons and the other protons in each ring.

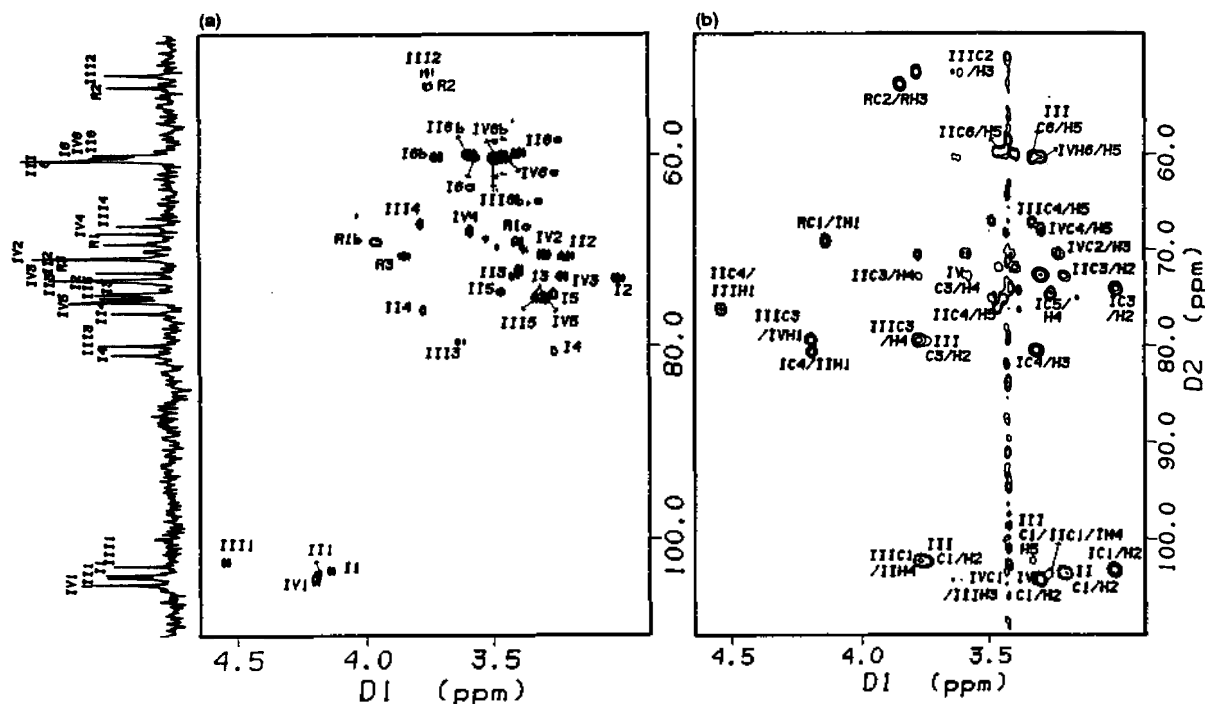


Figure 5. (a) Phase sensitive, ^{13}C -decoupled, ^1H detected multiple-quantum correlation (HMQC) spectrum of 7 mM G_{A1} in $\text{DMSO-}d_6\text{-D}_2\text{O}$ (98 : 2, v/v) at 303 K, at 500 MHz, showing the region of the ring carbons. Left side is the 1D carbon spectrum of G_{A1} . (b) HMBC spectrum of 7 mM G_{A1} in $\text{DMSO-}d_6\text{-D}_2\text{O}$ (98 : 2, v/v) at 303 K, at 500 MHz in magnitude mode, showing the same region.

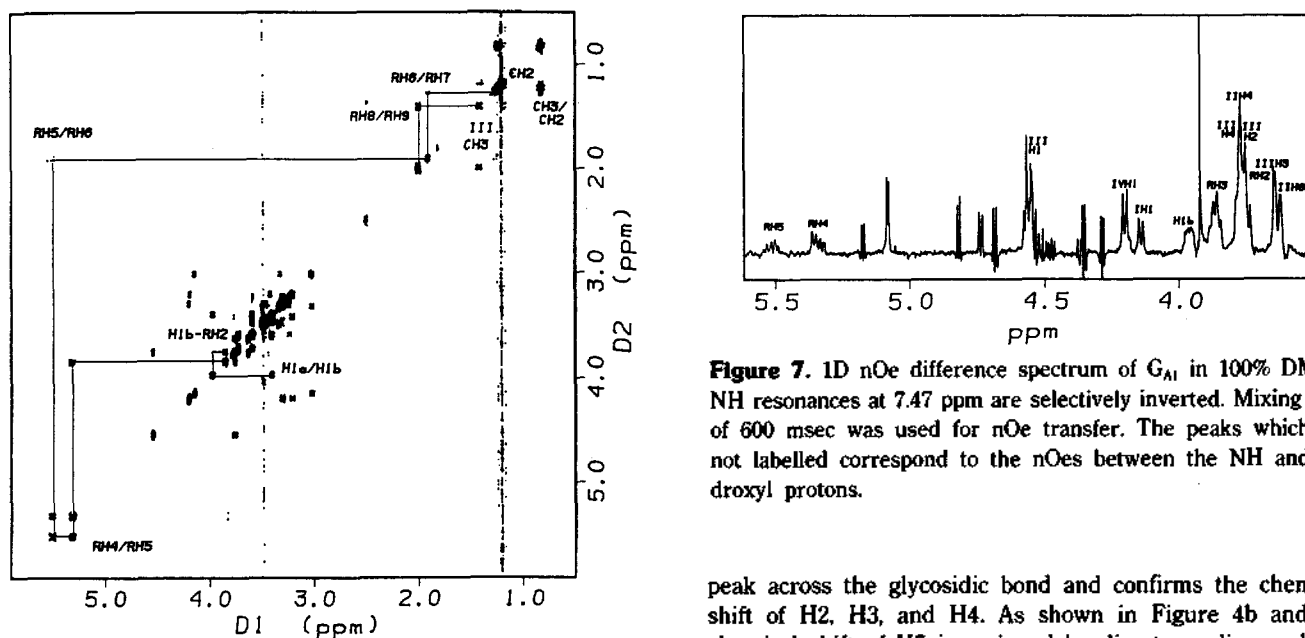


Figure 6. DQF-COSY spectrum of 7 mM G_{A1} in $\text{DMSO-}d_6\text{-D}_2\text{O}$ (98 : 2, v/v) at 303 K, at 500 MHz. Through-bond connectivities of protons in ceramide are shown with solid lines.

ric resonance (4.547 ppm) yielded proton assignment up to the H6b resonance of ring III. Assignment of H4 resonance (3.790 ppm) is complicated by the H2 resonance (3.758 ppm) and the IIIH2/H3 cross peak is overlapped with the IIIH4/H3 cross peak. HMBC spectrum shows the IVC1/IIIH3 cross

peak across the glycosidic bond and confirms the chemical shift of H2, H3, and H4. As shown in Figure 4b and 4c, chemical shift of H5 is assigned by direct coupling and the H1/H5 cross peak in NOESY spectrum. Especially, the C1/H5 cross peak shows up in the HMBC spectrum and helps to assign chemical shift of C5. Amide proton (7.479 ppm) shows a connectivity to H2 of this ring (3.758 ppm) in the DQF-COSY spectrum (data not shown). Intraring nOe connectivities from CH_3 to NH of N-acetyl group in the ring III makes it possible to assign the resonance of CH_3 .

As shown in Figure 4b, TOCSY spectrum shows cross peak connectivities from the anomeric proton at 4.199 ppm up to H6a resonances of ring IV. Chemical shifts of H2, H3,

Table 1. Assignment of ^1H Resonances of G_{A1} Obtained in $\text{DMSO-d}_6\text{-D}_2\text{O}$ (98 : 2, v/v) at 500 MHz and 303 K, Referenced to DMSO Signal at 2.49 ppm

| Residue Atom number | D-Glucose (I) | D-Galactose (II) | <i>N</i> -Acetyl-D-Galactosamine (III) | D-Galactose (IV) | Ceramide (R) |
|------------------------|---------------|------------------|--|------------------|--------------------|
| 1 | 4.142 | 4.196 | 4.547 | 4.199 | a: 3.405, b: 3.961 |
| 2 | 3.019 | 3.212 | 3.758 | 3.304 | 3.748 |
| 3 | 3.324 | 3.434 | 3.629 | 3.235 | 3.850 |
| 4 | 3.273 | 3.784 | 3.790 | 3.592 | 5.321 |
| 5 | 3.265 | 3.479 | 3.344 | 3.297 | 5.516 |
| 6 (a, b) | 3.586, 3.725 | 3.404, 3.596 | 3.497, 3.508 | 3.514, 3.592 | 1.907 |
| 7 | | | | | 1.273 |
| 8 | | | | | 2.001 |
| 9 | | | | | 1.426 |
| NH | | | 7.479 | | 7.463 |
| CH_2 | | | | | 1.209 |
| CH_3 | | | 1.813 | | 0.828 |

Table 2. Assignment of ^{13}C Resonances of G_{A1} Obtained in $\text{DMSO-d}_6\text{-D}_2\text{O}$ (98 : 2, v/v) at 500 MHz and 303 K, Referenced to DMSO Signal at 39.5 ppm

| Residue Atom number | D-Glucose (I) | D-Galactose (II) | <i>N</i> -Acetyl-D-Galactosamine (III) | D-Galactose (IV) | Ceramide (R) |
|------------------------|---------------|------------------|--|------------------|--------------|
| 1 | 103.529 | 103.812 | 102.593 | 104.546 | 69.253 |
| 2 | 73.181 | 70.789 | 51.696 | 70.680 | 52.990 |
| 3 | 74.365 | 73.025 | 79.790 | 72.973 | 70.789 |
| 4 | 80.778 | 76.428 | 67.358 | 68.120 | 131.363 |
| 5 | 74.891 | 74.568 | 75.244 | 75.342 | 131.676 |
| 6 | 60.252 | 59.986 | 60.610 | 60.512 | 31.354 |
| 7 | | | | | 22.145 |
| 8 | | | | | 35.698 |
| 9 | | | | | 25.473 |
| C=O | | | 170.937 | | 172.087 |
| CH_2 | | | | | 29.101 |
| CH_3 | | | 23.289 | | 13.971 |

and H4 were easily assigned by multiple relayed through-bond connectivities to H1 in TOCSY spectrum (Figure 4b) and through-space connectivities to H1 in NOESY spectrum (Figure 4c). Chemical shift of H5 is assigned by the C1/H5 cross peak in the HMBC spectrum and the C5/H5 cross peak in the HMQC spectrum. Resonances of H6a and H6b are assigned by HMQC and HMBC spectra.

Figure 6 is the DQF-COSY spectrum which shows the assignment of ceramide. The resonances up to RH9 methylene protons are well resolved in DQF-COSY and TOCSY spectrum. A cross section taken through the resonances from RH2 to the other protons up to RH7 in the 2D TOCSY spectrum confirms the assignment of protons up to RH7. Amide proton in ceramide shows the through-bond connectivities with RH2, RH3, RH4, H1a and H1b in DQF-COSY, RELAY and TOCSY spectra (data not shown). Every resonance in ceramide is confirmed by HMQC and HMBC spectra.

The complete assignment of proton and carbon resonances for G_{A1} is summarized in Table 1 and Table 2. All the carbon resonances are assigned as shown in Figure 5. Assignment

of ^{13}C NMR spectrum was necessary for assigning the complicated ^1H spectrum. The large chemical shift range of the ^{13}C -NMR spectra enabled us to resolve the resonances for most of carbon resonances of G_{A1} . However, like proton spectrum, carbon 1D spectrum suffers from spectral overlap between 60 and 80 ppm. Since G_{A1} is lack of polar sialic acid which perturbs the local nuclear field of the adjacent carbon and hydrogen atoms in the other gangliosides, spectrum of G_{A1} has severe spectral overlap compared to the spectrum of G_{M1} .¹¹ For the same reason, asialo-gangliosides can not be dissolved in polar solvent such as water and this is one of the reasons that $\text{DMSO-D}_2\text{O}$ (98 : 2, v/v) solvent was used in this study.

Lowest energy conformation of G_{D1a} which has two sialic acids shows that the internal, branched sialic acid is stacked underneath the GalNAc residue, establishing a hydrogen bond between the carboxyl group of the sialic acid and NH of the GalNAc unit.¹⁴ This hydrogen bond results in a rigidity of the branched sialic acid, while the terminal sialic acid appears to be more flexible. G_{M1} has intramolecular hydrogen

Table 3. NOEs for the NH protons in GalNAc and ceramide obtained from 2D NOESY spectrum (mixing time; 150 msec) and the 1D nOe spectrum (mixing time; 600 msec)

| Spectrum Residue | 2D NOESY | 1D nOe |
|---------------------|----------|--------|
| NH in GalNAc | IIH4 | IIH2 |
| | IIH1 | IIH4 |
| | IIH3 | IIH6b |
| | IVH1 | IIH1 |
| | | IIH2 |
| | | IIH3 |
| | IIH4 | |
| | IVH1 | |
| NH in ceramide | IH1 | IH1 |
| | H1a | H1a |
| | RH2 | H1b |
| | RH3 | RH2 |
| | RH8 | RH3 |
| | | RH4 |
| | RH5 | |

bonding between the NH of GalNAc unit and the carboxyl group of sialic acid and is stabilized energetically.¹¹ Even though G_{A1} does not have sialic acid to stabilize the conformation, NH in GalNAc (ring III) exchanges with deuterium slowly and appears to be involved in intramolecular hydrogen bond. Figure 7 shows the 1D nOe difference spectrum of G_{A1} in 100% DMSO. Since the chemical shifts of NH in GalNAc and NH in ceramide are very similar, both of NH resonances at 7.47 ppm are selectively inverted at the same time. Table 3 shows the nOe for the NH in GalNAc and NH in ceramide from 2D NOESY spectrum and 1D nOe spectrum. Amide proton in GalNAc shows many interring nOes with the protons in ring II and ring IV. According to this data, acetamido group in GalNAc (ring III) appears to be surrounded by ring II and ring IV and this may be an important factor in tertiary folding of G_{A1}. Further studies on this conformational property is going on.

The long-range ¹³C-¹H correlations across the glycosidic linkage by HMBC experiment is very helpful to assign the complicated proton resonances. Combination of proton 2D NMR experiments and heteronuclear proton-carbon correlation experiments makes it possible to complete the assignment of ¹H and ¹³C resonances of G_{A1}. These assignments will be useful for interpreting ¹H and ¹³C NMR data from uncharacterized oligosaccharides and for determining linkage position, the number of sugar rings, and the sequence of new ganglioside. Based on this assignment, determination of three dimensional structure of G_{A1} will be carried out.

Studies on the conformational properties of G_{A1} may lead to a better understanding of the molecular basis of its functions.

Acknowledgment. This work was financially supported by Korea Science and Engineering Foundation (94-1400-04-01-3).

References

1. Wiegandt, H. *Adv. Neurochem.* **1982**, *4*, 149.
2. Yoon, H.; Park, H.; Jhon, G. *Biochemistry Int.* **1992**, *28*, 393.
3. Fishman, P. H. In *New Trends in Ganglioside Research*; Ledeen, R. W.; Hogan, E. L.; Tettamanti, G.; Yates A. J.; Yu, R. K., Eds.; Liviana Press: Padova, Italy, 1988.
4. Kasai, M.; Iwamori, M.; Nagai, Y.; Okumura, K.; Tada, T. *Eur. J. Immunol.* **1980**, *10*, 175.
5. Young, W. W. Jr.; Hakamori, S.; Durdik, J. M.; Henney, C. S. *J. Immunol.* **1980**, *124*, 199.
6. Schwarting, G. A.; Summers, A. *J. Immunol.* **1980**, *124*, 1691.
7. Habu, S.; Kasai, M.; Nagai, Y.; Tamaoki, N.; Tada, T.; Herzenberg, L. A.; Okumura, K. *J. Immunol.* **1981**, *11*, 2.
8. Momoi, T.; Wiegandt, H.; Arndt, R.; Thiele, H. G. *J. Immunol.* **1980**, *125*, 2496.
9. Nakahara, K.; Ohashi, T.; Hirano, T.; Kasai, M.; Okumura, K.; Tada, T. *F. N. Engl. J. Med.* **1980**, *302*, 674.
10. Sillerud, L. O.; Yu, R. K. *Carbohydrate Research* **1983**, *113*, 173.
11. Acquotti, D.; Poppe, L.; Dabrowski, J.; Lieth, C.; Sonnino, S.; Tettamanti, G. *J. Am. Chem. Soc.* **1990**, *112*, 7772.
12. Scarsdale, J. N.; Prestegard, J. H.; Yu, R. K. *Biochemistry* **1990**, *29*, 9843.
13. Siebert, H.; Reuter, G.; Schauer, R.; Lieth, C.; Dabrowski, J. *Biochemistry* **1992**, *31*, 6962.
14. Sabesan S.; Duus, J. O.; Fukunaga, T.; Bock, K.; Ludvigsen, S. *J. Am. Chem. Soc.* **1991**, *113*, 3236.
15. Derome, A.; Williamson, M. *J. Magn. Reson.* **1990**, *88*, 177.
16. Bax, A.; D. G. *J. Magn. Reson.* **1985**, *65*, 355.
17. Macura, S.; Ernst, R. R. *Mol. Phys.* **1980**, *41*, 95.
18. Bodenhausen, G.; Ruben, D. J. *Chem. Phys. Lett.* **1980**, *69*, 185.
19. Aue, W. P.; Bartholdi, E.; Ernst, R. R. *J. Chem. Phys.* **1976**, *64*, 2229.
20. Nagayama, K. *J. Magn. Reson.* **1980**, *40*, 321.
21. Bax, A.; Freeman, R. *J. Magn. Reson.* **1981**, *44*, 542.
22. Bax, A.; Subramanian, S. *J. Magn. Reson.* **1986**, *67*, 565.
23. Bax, A.; Summers, M. F. *J. Am. Chem. Soc.* **1986**, *108*, 2093.
24. Bax, A.; Davis, D. G. *J. Magn. Reson.* **1985**, *63*, 207.
25. Biosym technologies, Inc.; Sandiego, CA.